Surface Simplex Meshes for 3D Medical Image Segmentation

Johan Montagnat, Hervé Delingette, Nicolas Scapel, Nicholas Ayache

Surface Simplex Meshes for 3D Medical Image Segmentation

J. Montagnat, H. Delingette, N. Scapel and N. Ayache

Epidaure Project
I.N.R.I.A., 06902 Sophia-Antipolis Cedex, BP 93, France
http://www-sop.inria.fr/epidaure/ - Nicholas.Ayache@sophia.inria.fr

Abstract

Medical image segmentation is often a difficult task due to the low contrast, the low signal/noise ratio and the presence of outliers in images. However, it remains a critical issue for image interpretation, pattern recognition and automatic diagnosis. Deformable models are well-suited for capturing the geometry and the shape variability of anatomical structures from medical images. Indeed, they introduce an a priori *knowledge in the segmentation process that increases its robustness to noise and outliers. In this paper, we address many problems related to volumetric medical image segmentation based on deformable models including model initialization, model topology, deformation behavior and image features extraction.*

1 Introduction

For the past decade, there has been a significant research effort for achieving medical image segmentation based on deformable models. The main incentive behind this research is to provide reliable segmentation tools that are both robust and generic.

A wide variety of surface representations and evolution frameworks have been proposed in the literature [13]. For instance, deformable models were introduced by Kass *et al* as 2D explicit deformable contours [9] and generalized to the 3D case by Terzopoulos *et al.* [20]. Parametric representations such as superquadrics [21, 2] and discrete representations [16, 8] have also been proposed. Recently, implicit representations have been used with the ability to handle topology changes [11, 22, 10].

When considering the segmentation of medical images, the basic idea is to steer deformable models towards the image structure boundaries. Due to the image noise and the lack of contrast between structures in many image acquisition systems [1], it is in general needed to constrain the model variation space and to introduce some *a priori* information during the deformation process. For instance, statistical shape variations from a training set [6] may be used to constrain the deformation of a geometric model.

In this paper, we introduce a discrete surface representation called *simplex meshes*. It provides a simple geometric representation combined with a powerful framework for regularization (section 2). In section 3, we propose several methods to achieve shape regularization which is a key issue of deformable modeling. We consider local regularizing constraints designed to ensure local surface regularity whether prior information on the expected anatomical structures shape is available or not. We also constrain the deformations at a global scale to make the segmentation process robust to outliers and false positives. In section 4, we propose an automatic model initialization method to generate a surface mesh from an image with the desired shape and topology. We show how to use topology operators on discrete meshes to allow surface resampling as well as changes in the surface genus (section 5). Finally, we use simplex meshes for medical image segmentation in section 6. Various image geometries as well as image acquisition modalities are considered. Heart left ventricle segmentation from 3D ultrasound images are shown.

2 Simplex Mesh Representation

A simplex mesh $\mathcal{M}$ is defined by a set of vertices $\{\mathbf{p}_i\}_i$ and a specific connectivity function. Each vertex of a k-simplex mesh is connected to exactly $k+1$ neighbors. A 1-simplex mesh is a simple deformable contour composed of a polygonal line. A 2-simplex mesh is a deformable surface for which each vertex is connected to exactly three neighbors. A detailed description of simplex meshes is given in [8].

2.1 Geometry

Due to its specific connectivity, a 2-simplex mesh is topologically dual to a triangulation. Figure 1 (left) shows a 2-simplex mesh example (solid line) and a dual triangulation (dashed line).

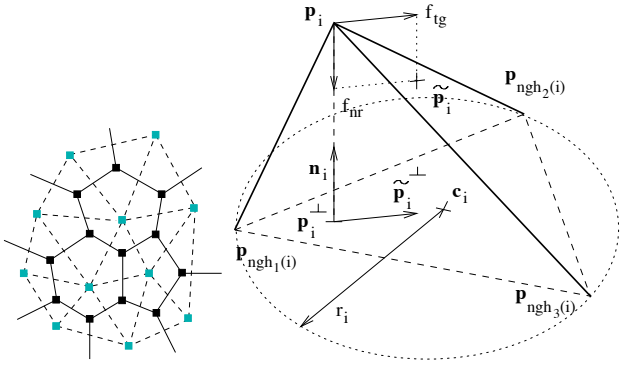

Figure 1: (Right) 2-simplex mesh duality with triangulations; (Left) Geometry and definition of the regularizing force.

The main features of simplex meshes lies in their simple geometric description. Figure 1 (right) shows a vertex $\mathbf{p}_i$ of a 2-simplex mesh and its three neighbors, $\mathbf{p}_{\mathrm{ngh}_j(i)}$. Let $\mathcal{P}_i$ be the plane defined by $\mathbf{p}_i$'s three neighbors. We denote $\mathbf{p}_i^\perp$ the projection of $\mathbf{p}_i$ on $\mathcal{P}_i$ and $\mathbf{n}_i$ the unit normal vector of $\mathcal{P}_i$. We introduce the circumscibed circle to triangle $(\mathbf{p}_{\mathrm{ngh}_1(i)}, \mathbf{p}_{\mathrm{ngh}_2(i)}, \mathbf{p}_{\mathrm{ngh}_3(i)})$ with center $\mathbf{c_i}$ and radius r_i, and the circumscribed sphere to vertices $(\mathbf{p}_i, \mathbf{p}_{\mathrm{ngh}_1(i)}, \mathbf{p}_{\mathrm{ngh}_2(i)}, \mathbf{p}_{\mathrm{ngh}_3(i)})$ with center $\mathbf{o_i}$ and radius R_i.

We call *metric parameters* the barycentric coordinates ε_i^1, ε_i^2, and $\varepsilon_i^3 = 1 - \varepsilon_i^1 - \varepsilon_i^2$ of $\mathbf{p}_i^\perp$ with respect to $\mathbf{p}_i$'s neighbors. They control the relative position of $\mathbf{p}_i^\perp$ in $\mathcal{P}_i$. The *simplex angle* $\varphi_i \in [-\pi, \pi]$ is defined by :

$$\sin(\varphi_i) = \frac{r_i}{R_i}\mathrm{sign}((\mathbf{p}_{\mathrm{ngh}_1(\mathrm{i})} - \mathbf{p_i}) \cdot \mathbf{n_i})$$

$$\cos(\varphi_i) = \frac{\|\mathbf{c_i} - \mathbf{o_i}\|}{R_i}\mathrm{sign}((\mathbf{c_i} - \mathbf{o_i}) \cdot \mathbf{n_i}).$$

It controls the elevation of vertex $\mathbf{p}_i$ above $\mathcal{P}_i$. We define a vertex discrete mean curvature as $H_i = \frac{1}{R_i} = \frac{\sin(\varphi_i)}{r_i}$. Under some assumptions it can be shown that the discrete curvature of a mesh whose vertices lie on a continuous and sufficiently differentiable surface converges towards the surface mean curvature.

The vertex position $\mathbf{p}_i$ is uniquely defined by its three neighbors, its metric parameters and its simplex angle :

$$\mathbf{p}_i = \left(\sum_{j=1}^{3} \varepsilon_i^j \mathbf{p}_{\mathrm{ngh}_j(i)}\right) + H(\mathbf{p}_{\mathrm{ngh}_j(i)}, \varepsilon_i^j, \varphi_i)\mathbf{n}_i.$$

$$H = \frac{(r_i^2 - d_i^2)tan(\varphi_i)}{\epsilon\sqrt{r_i^2 + (r_i^2 - d_i^2)tan(\varphi_i)^2} + r_i}$$

$$\epsilon = \begin{cases} 1 \text{ if } |\varphi_\mathbf{i}| < \frac{\pi}{2} \\ -1 \text{ if } |\varphi_\mathbf{i}| > \frac{\pi}{2} \end{cases}, \quad d_i = \|\mathbf{p}_i^\perp \mathbf{c_i}\|$$

It can be shown that a simplex mesh shape is defined up to a similarity transformation by the set of its metric parameters and simplex angles $\{\varepsilon_i^1, \varepsilon_i^2, \varphi_i\}_i$.

2.2 Law of motion

In a 2-simplex mesh, each vertex is submitted to a regularizing, or internal force ($\mathbf{f}_{\mathrm{int}}$) dependent on the surface geometry and a data attraction, or external force ($\mathbf{f}_{\mathrm{ext}}$). The vertex $\mathbf{p}_i$ is considered as a physical mass evolving according to a Newtonian law of motion :

$$m_i \frac{d^2\mathbf{p}_i}{dt^2} = -\gamma \frac{d\mathbf{p}_i}{dt} + \mathbf{f}_{\mathrm{int}}(\mathbf{p}_i) + \mathbf{f}_{\mathrm{ext}}(\mathbf{p}_i), \qquad (1)$$

where m_i and γ are respectively the vertex mass and a damping parameter. Equation 1 is discretized in time using finite differences with an explicit scheme :

$$\mathbf{p}_i^{t+1} = \mathbf{p}_i^t + (1-\gamma)(\mathbf{p}_i^t - \mathbf{p}_i^{t-1}) + \alpha_i \mathbf{f}_{\mathrm{int}}(\mathbf{p}_i^t) + \beta_i \mathbf{f}_{\mathrm{ext}}(\mathbf{p}_i^t),$$

where α_i and β_i are force weights including the vertex mass and the time step. The stability of this scheme is guaranteed if α_i and β_i are below a given threshold.

3 Regularization

Shape regularization is a key issue in deformable modeling. Regularization of the deformation process can be controlled at different scales.

3.1 Local regularization

Due to its discrete nature, the regularization of a simplex mesh is not based on the evaluation of surface partial derivatives but on the relative position of a vertex with respect to its neighbors, i.e. in terms of metric parameters and simplex angles. More precisely, each vertex $\mathbf{p}_i$ is attracted towards a point $\tilde{\mathbf{p}}_i$ (see figure 1, right) on a smoother mesh. Let $\tilde{\varepsilon}_i^j$, $\tilde{\varphi}_i$ and $\tilde{\mathbf{p}}_i^\perp$

denote the metric parameters, the simplex angle and the projection of $\tilde{\mathbf{p}}_i$ on $\mathcal{P}_i$ respectively. The internal force can be decomposed as the sum of a tangential and normal component :

$$\mathbf{f}_{\text{int}}(\mathbf{p}_i) = \mathbf{f}_{\text{tg}}(\mathbf{p}_i) + \mathbf{f}_{\text{nr}}(\mathbf{p}_i) = (\tilde{\mathbf{p}}_i^{\perp} - \mathbf{p}_i^{\perp}) + (H(\mathbf{p}_{\text{ngh}_j(i)}, \varepsilon_i^j, \varphi_i) - H(\mathbf{p}_{\text{ngh}_j(i)}, \tilde{\varepsilon}_i^j, \tilde{\varphi}_i))\mathbf{n}_i.$$

The tangential component of the internal force controls the vertex spacing over the surface. To ensure uniformly spread vertices, metric parameters are all set equal : $\tilde{\varepsilon}_i^1 = \tilde{\varepsilon}_i^2 = \tilde{\varepsilon}_i^3 = \frac{1}{3}$. The normal component constrains the mean curvature of the surface through the simplex angle. The definition of $\tilde{\varphi}_i$ depends on the level of geometric regularity that should be enforced.

Let $\mathcal{N}_s(i)$ be the set of all vertices connected to vertex number i by an edges path whose length is less than s edges. The scale parameter, s, defines the neighborhood size over which the mesh is regularized and plays an important role. For medical image segmentation we usually consider :

- *Mean curvature continuity.* To ensure that the vertex discrete mean curvature converges towards the weighted average mean curvature of its neighborhood, we set

$$\tilde{\varphi}_i = \arcsin\left(\mathrm{r_i} \sum_{\mathrm{j}\in\mathcal{N}_s(\mathrm{i})} \mathrm{e_{ij}} \frac{\sin(\varphi_\mathrm{j})}{\mathrm{r_j}}\right), \sum_{\mathrm{j}\in\mathcal{N}_s(\mathrm{i})} \mathrm{e_{ij}} = 1.$$

  This smoothness constraint should be used when no anatomical shape information is available.

- *Shape constraint.* Let $\{\varphi_i^\circ\}_i$ be the set of simplex angles defining the reference shape of an anatomical structure. Setting $\tilde{\varphi}_i = \varphi_i^\circ$ constrains the surface to converge towards the reference shape in the abscence of external forces. This constraint should be used when an *a priori* shape information is available.

3.2 Global regularization

In general, the convergence of the deformation process is very sensitive to the model initial shape and orientation. One approach proposed by Besl and McKay [3] is to iteratively apply a global transformation T that minimizes a least-square criterion. This criterion corresponds to the distance of the deformed model to a set of boundary points. With the notation introduced previously, the optimal transformation T is :

$$T = \arg\min_{T\in\mathrm{T_{reg}}} \sum_{\mathbf{p}_i\in\mathcal{M}} \|T(\mathbf{p}_i) - (\mathbf{p}_i + \beta_i \mathbf{f}_{\text{ext}}(\mathbf{p}_i))\|^2 \quad (2)$$

where $\{\mathbf{f}_{\text{ext}}(\mathbf{p}_i)\}_i$ is the set of displacement vectors of vertices towards boundary points and $\mathrm{T_{reg}}$ is a given group of transformations with a limited number of degrees of freedom (DOF). Widely used transformation groups include rigid transformations (6 DOF), similarities (7 DOF) and affine transformations (12 DOF). For these three transformation groups, there exists a closed form solution for solving equation 2.

By restricting the transformation in $\mathrm{T_{reg}}$, this algorithm improves the robustness to noise and outliers of the image segmentation. Therefore, this approach tends to be less sensitive to the initial model position than classical deformable model approaches. However, its drawback is to limit the possible range of model deformations. It may not allow to describe the complex shape variability of anatomical structures.

3.3 From local to global regularization

Many approaches have been proposed to combine a global deformation procedure limiting the model shape variations and a local deformation component to match small shape variations [21, 18, 19]. In [14], we introduce a computationally efficient scheme combining a global transformation estimation and local deformations. The global transformation T is converted to a global and regular force field : $\mathbf{f}_{\text{global}}(\mathbf{p}_i) = T(\mathbf{p}_i) - \mathbf{p}_i$. The surface is submitted to internal, external and global forces. A *locality* parameter λ allows to weight the influence of each force :

$$\mathbf{p}_i^{t+1} = \mathbf{p}_i^t + (1-\gamma)(\mathbf{p}_i^t - \mathbf{p}_i^{t-1}) + \lambda(\alpha_i \mathbf{f}_{\text{int}}(\mathbf{p}_i^t) + \beta_i \mathbf{f}_{\text{ext}}(\mathbf{p}_i^t)) + (1-\lambda)\mathbf{f}_{\text{global}}(\mathbf{p}_i^t). \quad (3)$$

From equation 3 it can be seen that when $\lambda = 0$, the deformations are purely global, and when $\lambda = 1$, the deformations are only local. Any other value of λ leads to an intermediate behavior. This approach is efficient since external forces are computed only once for local and global forces estimation. The global transformation is estimated using a closed form solution.

This method allows a "coarse-to-fine" approach similar to the Graduated Non-Convexity algorithm [4]. When λ is 0, the deformation problem is rather convex and the convergence is robust. As λ increases, several local minima appear until the original (local) equation is used. At each iteration, the current deformation optimum is used as an initialization for the model.

4 Initialization

The initialization of deformable models has often been considered as the main limitation of that approach. In some medical applications, it is possible to estimate a prior shape and orientation of the anatomical structure of interest, knowing the patient orientation inside the acquisition device. Global transformations may then be used to compensate for the small orientation and scale variations between a rough initialization and the patient image.

Nevertheless, it may happen that the initial position and/or shape of the anatomical structure is not known. We then propose an automatic procedure to build a simplex mesh directly from the volumetric image [7]. First, the image needs to be binarized, using thresholding and mathematical morphology operators, to reveal a rough approximation of the structure of interest. A two stages algorithm is used to initialize the mesh from the binary image. Figure 2 (left) shows an example on an MR Image of the hand.

- A surface tracking algorithm first extracts a surface from the object boundary voxels (center). The resulting surface needs to be a discrete 2D manifold.

- A sampling algorithm preserving the surface topology then produces a mesh at a given resolution. It propagates regions from randomly selected seeds over the surface. By splitting regions when needed, a simplex mesh is created. The result is obtained by adapting the mesh topology to the desired level of detail and deforming the mesh in the original image (right).

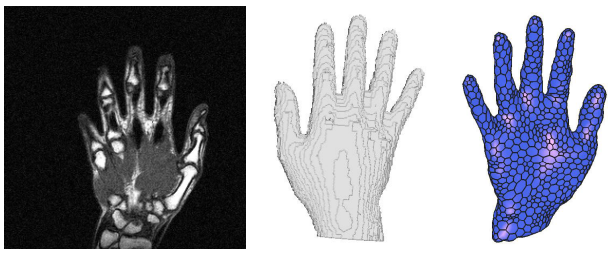

Figure 2: Simplex mesh automatic initialization in an MR Image of a hand.

5 Topology

Topology adaptation of deformable models is an important feature when the datasets are reliable enough to allow an automatic detection of topology changes. Discrete mesh topology operators include both mesh resampling (Eulerian operations) and changes in the surface genus (non-Eulerian operations).

5.1 Surface adaptation and refinement

Mesh sampling is key to control the model level of detail. In general, one wants to minimize the size of the geometric representation (a compact model) with sufficient details to represent the finest image structures. We developed topology operators allowing to locally refine or decimate a simplex mesh surface [17].

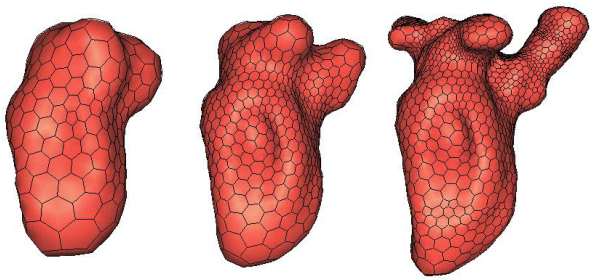

Figure 3: Surface refinement for heart and vessels segmentation

Figure 3 shows the segmentation of a dog's heart and blood vessels from a CT-scan starting from a spherical model. From left to right the model is refined based on its local discrete curvature; it consists of approximatively 500, 1500 and 5000 vertices.

5.2 Topology changes

Automatically adapting a surface genus during the deformation process is a challenging issue. The implicit representation (level set) is well-suited to topology changes since no surface parameterization is required. However, level sets suffer from other limitations such as the difficulty for user interaction and its expensive computing time. McInerney and Terzopoulos proposed the «T-snakes» models [12] to apply topology changes on discrete contours and surfaces, based on the decomposition of space on a simplicial grid. We propose an algorithm for automatically performing topology changes on 1-simplex meshes. It

is also based on a decomposition of space on a regular grid, although it is not restricted to close contours as T-snakes. Figure 4 shows a circular topology deformable contour segmenting a vertebra. The contour is pushed by a balloon force to grow until it locks on edges. New vertices are created when needed and the contour self-intersects resulting in a split into two connected components.

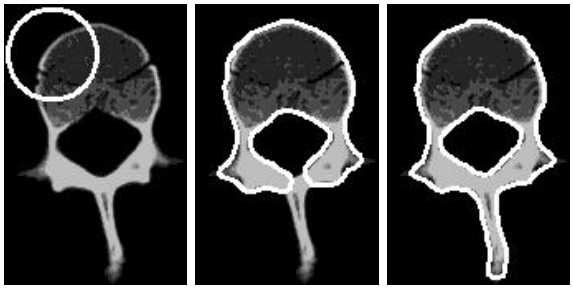

Figure 4: Topology adaptable snake

6 Medical images segmentation

.

6.1 Image geometry

Most medical images are sampled along a regular grid in Euclidian space. However, some acquisition devices acquire volumetric images using different geometries. In particular, 3D ultrasound probes often acquire a set of 2D planes that may not be parallel to each other. Figure 5 shows a rotative ultrasound probe and the corresponding cylindrical sampling grid. In these images, the data density decreases as a function of the distance to the symmetry axis. In [15] we proposed an algorithm for filtering images with a non Euclidian geometry. This is especially useful to extract gradient information which is the main feature used for image segmentation.

6.2 External forces

Although the use of global deformations improves the segmentation robustness, high segmentation accuracy can be achieved by introducing some specific knowledge about the structures of interest.

External forces are computed from an image I to push a deformable model towards anatomical structure boundaries. In their seminal paper [9], Kass *et al*

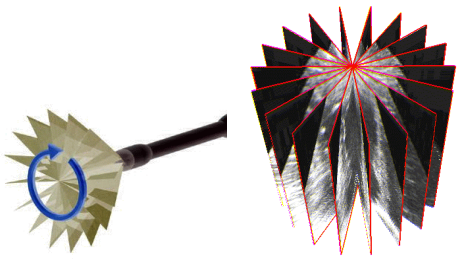

Figure 5: A rotative ultrasound probe and the resulting cylindrical geometry image. This image was acquired at the CHU Brabois by Dr Lethor for the Échocard3D project.

proposed to use the gradient of the image gradient's norm as the external force : $\mathbf{f}_{\text{ext}} = \nabla\|\nabla I\|$. The potential field associated with this force tends to be fairly narrow around image edges. Moreover, the model evolution might become unstable. Cohen [5] proposed a normalization to avoid instabilities and adds a balloon force that causes the model inflation. The use of a function of the distance from a model vertex to the edge points also avoids instabilities. Thus forces computation often requires the extraction of main edges. A distance map is then computed from the edges or a closest edge point is determined for each model vertex.

6.2.1 Gradient based forces

We use different external forces depending on the image quality and specificity. For most CT and MR images, the contrast is high enough to extract boundaries using a gradient operator. The model then tracks close boundaries at each pixel by scanning image voxels along the normal direction at each vertex. The scan-line algorithm is illustrated for Euclidian and cylindrical images in figure 6. Restricting the boundary search along the model normals reduces the scanning time without limiting the deformation capabilities.

If the scan-line from a vertex intersects a voxel of high gradient norm, the external force is computed as the displacement vector from the vertex position to the boundary voxel center. To make the boundary detection more robust, several criteria can be taken into account :

- *Range.* The scan-line algorithm scans voxels within a limited range to avoid reaching outliers when gradient voxels are lacking. The range parameter is either dependent on the image size or of the average structure size when it is known.

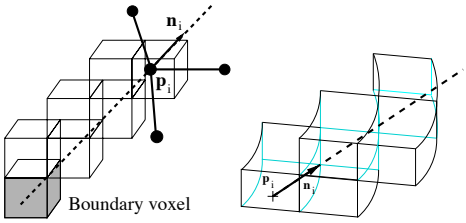

Figure 6: Scan-line algorithm for different image geometries.

- *Contrast.* In fairly well contrasted images, a lower gradient intensity threshold can be set to ignore voxels whose gradient's norm is too low (weak contours or noise).
- *Direction.* If the segmented structure is brighter or darker than the image background, the gradient vector is always pointing outside or inside that structure. A gradient voxel found on a vertex normal line is rejected if its direction does not roughly match the normal direction.
- *Intensity.* Finally, if the structures of interest intensity range is known, a gradient voxel can be rejected when the corresponding intensity voxel does not fall within the expected range.

6.2.2 Region based forces

In many cases, the gradient information may be lacking or the noise level may be too high to detect proper boundaries using a gradient operator. Moreover, gradient information is not necessarily relevant in some image acquisition systems, e.g. thick lines appear in ultrasound images along organ interfaces. An information on the gray-level distribution is then more appropriate.

We have developed an intensity region external force [15]. At each mesh vertex, an intensity profile is acquired from the image in the vertex normal direction. The profile is then smoothed using anisotropic diffusion to reduce noise without altering intensity discontinuities. When an homogeneous region (i.e. a profile segment with its voxels belonging to a given intensity range) having a minimum length is found, we search for voxels of high gradient in the vicinity of the region's extremities. These voxels correspond to the region boundary and are used to compute the external force.

Figure 7 shows the heart left ventricle segmentation from a time series of very noisy 3D ultrasound images with weak contours based on region-defined external forces. On the left, the reconstructed 3D model embedded in the original image is displayed. Two images of the model intersection with one image slice at end diastole (center) and end systole (right) are shown.

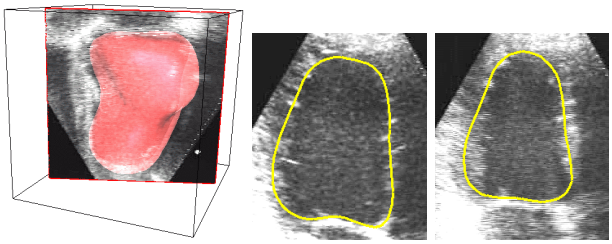

Figure 7: Segmentation of a 3D cardiac ultrasound images sequence.

7 Conclusion

Deformable surfaces provide a powerful tool for generic image segmentation. They produce a geometric representation of anatomical structures suited to visualization, quantitative measurements, surgery planning and simulation. Although deformable models may be trapped by local minima of the energy functional, their robustness is increased in many applications by the introduction of *a priori* information. Finally, these models can describe a wide variety of shapes without any restriction of topology.

Our future work will concentrate on extending the application field of image segmentation based on deformable models. For instance, the segmentation of time series of medical images is of high importance for many medical procedures including cardiology. We are developing time-dependent deformable models in order to obtain time-correlated image segmentation. Also, the reconstruction of vascular trees based on deformable models is challenging because of their complex geometry and tubular symmetry.

References

[1] R. Acharya, R. Wasserman, J. Sevens and C. Hinojosa, "Biomedical Imaging Modalities: a Tutorial", *Computerized Medical Imaging and Graphics*, Vol. 19(1), pp 3-25, 1995.

[2] E. Bardinet, L. Cohen, and N. Ayache, "Tracking and motion analysis of the left ventricle with de-

formable superquadrics", *Medical Image Analysis*, Vol. 1(2), pp 129-149, 1996.

[3] P. Besl and N. McKay, "A method for registration of 3D shapes", *IEEE Transactions on Pattern Analysis and Machine Intelligence*, Vol. 14(2), pp 239-256, 1992.

[4] A. Blake and A. Zisserman, "Visual Reconstruction", MIT Press, ISBN 0-262-02271-0, 1987.

[5] L.D. Cohen, "On Active Contour Models and Balloons", *Computer Vision, Graphics, and Image Processing: Image Understanding*, Vol. 53(2), pp 211-218, 1991.

[6] T.F. Cootes, C.J. Taylor, D.H. Cooper and J. Graham, "Active shape models, their training and application", *Computer Vision and Image Understanding*, Vol. 61(1), pp 38-59, 1995.

[7] H. Delingette, "Initialization of deformable models from 3D data", *International Conference on Computer Vision*, pp 311-316, Bombay, India, 1998.

[8] H. Delingette, "General Object Reconstruction based on Simplex Meshes", *International Journal of Computer Vision*, Vol. 32(2), pp 111-146, 1999.

[9] M. Kass, A. Witkin and D. Terzopoulos, "Snakes: Active Contour Models", *International Journal of Computer Vision*, Vol. 1, pp 321-331, 1988.

[10] L. Lorigo, O. Faugeras, W. Grimson, R. Keriven, R. Kikinis and C.-F. Westin, "Co-dimension 2 Geodesic Active Contours for MRA Segmentation", *International Conference on Information Processing in Medical Images*, Visegrád, Hungary, 1999.

[11] R. Malladi, J.A. Sethian, and B.C. Vemuri, "Shape Modeling with Front Propagation : A Level Set Approach", *IEEE Transactions on Pattern Analysis and Machine Intelligence*, Vol. 17(2), pp 158–174, 1995.

[12] T. McInerney and D. Terzopoulos, "Medical Image Segmentation using Topologically Adaptable Snakes", *Joint Conference on Computer Vision, Virtual Reality and Robotics in Medicine*, Grenoble, France, pp 92-100, 1997.

[13] T. McInerney and D. Terzopoulos, "Deformable Models in Biomedical Images", *Medical Image Analysis*, Vol. 1(2), pp 91-108, 1996.

[14] J. Montagnat and H. Delingette, "Globally constrained deformable models for 3D object reconstruction", *Signal Processing*, Vol. 71(2), pp 173-186, 1998.

[15] J. Montagnat, H. Delingette and G. Malandain, "Cylindrical Echocardiographic Images Segmentation based on 3D Deformable Models", *Medical Image Computing and Computer-Assisted Intervention*, Cambridge, UK, 1999.

[16] C. Nastar and N. Ayache, "Frequency-Based Nonrigid Motion Analysis: Application to Four Dimensional Medical Images", *IEEE Transactions on Pattern Analysis and Machine Intelligence*, Vol. 18(11), pp 1067-1079, 1996.

[17] Scapel, N. "Optimisation topologique et géométrique d'un maillage surfacique dynamique", *master thesis report*, INRIA, july 1999.

[18] L. Staib and J. Duncan, "Deformable Fourier models for surface finding in 3D images", Visualization in Biomedical Computing, pp 90-104, 1992.

[19] G. Székely, A. Kelemen, C. Brechbüler and G. Gerig, "Segmentation of 2D and 3D objects from MRI volume data using constrained elastic deformations of flexible Fourier surface models", *Medical Image Analysis*, Vol. 1(1), pp 19-34, 1996.

[20] D. Terzopoulos, A. Witkin and M. Kass, "Constraints on Deformable Models: Recovering 3D Shape and Nonrigid Motion", *Artificial Intelligence*, Vol. 36(1), pp 91-123, 1988.

[21] D. Terzopoulos and D. Metaxas, "Dynamic 3D Models with Local and Global Deformations: Deformable Superquadrics", *IEEE Transactions on Pattern Analysis and Machine Intelligence* Vol. 13(7), pp 703-714, 1991.

[22] X. Zeng, L. Staib, R. Schultz and J. Duncan, "Segmentation and Measurement of the Cortex from 3D MR Images", *Medical Image Computing and Computer-Assisted Intervention*, Cambridge, USA, 1998.